



PERGAMON

Polyhedron 20 (2001) 755–765



POLYHEDRON

www.elsevier.nl/locate/poly

Mixed halide/phosphine complexes of the dirhenium core. Part 7. Reactions of $[\text{Re}_2\text{I}_8]^{2-}$ with monodentate phosphines[☆]

Panagiotis Angaridis, F. Albert Cotton *, Evgeny V. Dikarev, Marina A. Petrukhina

*Laboratory for Molecular Structure and Bonding, P.O. Box 30012, Department of Chemistry, Texas A&M University,
College Station, TX 77842-3012, USA*

Received 13 March 2000; accepted 18 April 2000

Abstract

Reactions of the octaiododirhenate anion $[\text{Re}_2\text{I}_8]^{2-}$ with monodentate phosphines ($\text{PR}_3 = \text{PMe}_3$ (**1**), PMe_2Ph (**2**), PEt_3 (**3**), and PEt_2Ph (**4**)) have been studied in two different solvents, ethanol and benzene, at room temperature. The reactions in ethanol resulted in two-electron reduction products having the Re_2^{4+} core, $\text{Re}_2\text{I}_4(\text{PR}_3)_4$ ($\text{R}_3 = \text{Me}_3$ (**1a**) and Me_2Ph (**2a**)), for which X-ray diffraction study revealed a 1,3,6,8 isomer type. The reaction of $[\text{Re}_2\text{I}_8]^{2-}$ with PMe_3 in benzene led to an intermediate edge-sharing bioctahedral dirhenium(III) complex, $\text{Re}_2(\mu\text{-I})_2\text{I}_4(\text{PMe}_3)_4$ (**1b**), with no metal–metal bond. The interaction of PEt_3 with $[\text{Re}_2\text{I}_8]^{2-}$ in benzene again yielded a kinetic product with a different stoichiometry and a Re_2^{5+} core, $[\text{Bu}_4\text{N}][\text{Re}_2\text{I}_6(\text{PEt}_3)_2]$ (**3c**). The analogous reactions of $[\text{Re}_2\text{I}_8]^{2-}$ with PMe_2Ph and PEt_2Ph in benzene involved two-electron reductions and gave complex **2a** and $\text{Re}_2\text{I}_4(\text{PEt}_2\text{Ph})_4$ (**4a**), as products. Reduction of **1b** with KC_8 gave **1a** as the main product along with a few crystals of 1,3,6- $\text{Re}_2\text{I}_5(\text{PMe}_3)_3$ (**1d**). Mixed iodide/phosphine complexes of the dirhenium core Re_2^{n+} , where $n = 4$ (**1a**, **2a**, **4a**), 5 (**1d**, **3c**), and 6 (**1b**) have for the first time been characterized by X-ray crystallography. In addition, these products have been further identified by a combination of mass spectrometry and cyclic voltammetric measurements. © 2001 Published by Elsevier Science Ltd.

Keywords: Dirhenium complexes; Phosphine complexes; Iodides; Crystal structures; Metal–metal bonds; Edge-sharing bioctahedral complexes

1. Introduction

The chemistry and reactivity of the $[\text{Re}_2\text{I}_8]^{2-}$ ion is much less developed [1] than that of $[\text{Re}_2\text{Cl}_8]^{2-}$. It was noticed earlier that reactions of these two octahalodirhenate anions with monodentate phosphine ligands proceed differently [2]. The octaiododirhenate (III) anion upon reaction with tertiary phosphines in ethanol or acetone at room temperature affords two-electron reduction products $\text{Re}_2\text{I}_4(\text{PR}_3)_4$ ($\text{R} = \text{Et}$, Pr^n , Bu^n) [2] within a few minutes. The structures of those compounds have not been reported, although some spectroscopic and electrochemical characteristics were measured [3]. Analogous reactions of $[\text{Re}_2\text{Cl}_8]^{2-}$ re-

quire prolonged reflux to give the Re_2^{4+} core products, 1,3,6,8- $\text{Re}_2\text{Cl}_4(\text{PR}_3)_4$ (Scheme 1). In addition, depending on the choice of reaction conditions (temperature, time, solvent, concentration of Cl^- anions) mixed chloride/phosphine complexes of the Re_2^{6+} and Re_2^{5+} cores of types $\text{Re}_2\text{Cl}_6\text{P}_2$ and $\text{Re}_2\text{Cl}_5\text{P}_3$ (Scheme 1) can be produced [4,5]. These stoichiometries have not yet been seen for the iodides.

We have recently reported on the reactivity of the $[\text{Re}_2\text{Cl}_8]^{2-}$ ion toward a number of monodentate phosphines [5] that vary in basicity and cone angle. These studies led to the discovery of a new stereochemistry (1,2,7,8 or *cis, cis*; Scheme 1) for the type $\text{Re}_2\text{Cl}_4(\text{PR}_3)_4$ ($\text{R}_3 = \text{Me}_3$ [5a], Me_2Ph [5b] and Et_2H [5c]), which can be preserved under very mild experimental conditions. We also found different reaction pathways when the reactions of $[\text{Re}_2\text{Cl}_8]^{2-}$ with PMe_3 , PEt_3 and PPR_3^n were carried out in ethanol/acetone and benzene media [5a,e]. In ethanol/acetone the reduction process was found to proceed smoothly, while in benzene a dispro-

[☆] This article was presented at the Second Contemporary Inorganic Chemistry Conference (CIC-II) held at Texas A&M University, College Station, TX, USA, on March 12–15, 2000.

* Corresponding author. Tel.: +1-979-8454432; fax: +1-979-8459351.

E-mail address: cotton@tamu.edu (F.A. Cotton).

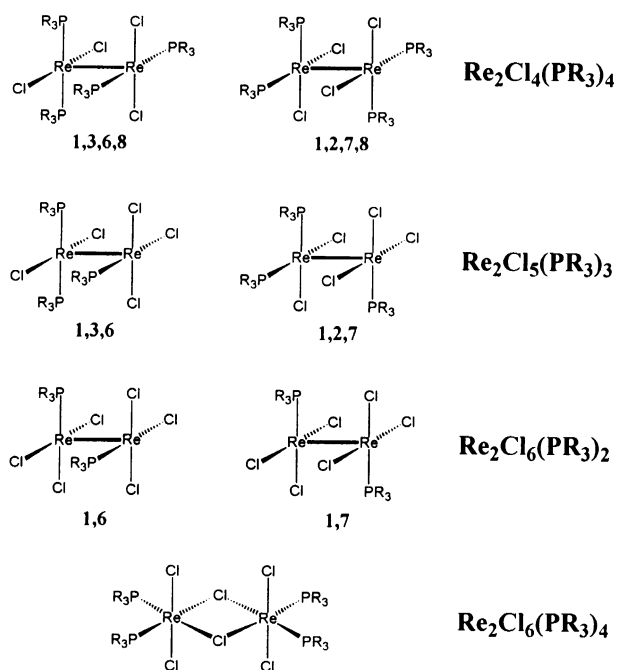
portionation mechanism, $3\text{Re}_2^{6+} \rightarrow 2\text{Re}^{4+} + 2\text{Re}_2^{5+}$, was confirmed and several intermediate species, including an edge-sharing bioctahedral complex of the type $\text{Re}_2\text{Cl}_6\text{P}_4$ (Scheme 1) were observed and isolated.

In view of the very extensive chemistry that arose from the reactions of phosphines with $[\text{Re}_2\text{Cl}_8]^{2-}$ under various conditions, and bearing in mind that from the early work of Walton and coworkers [2,3] the $[\text{Re}_2\text{I}_8]^{2-}$ ion might be expected to display both similarities and differences, we thought it worthwhile to explore further the chemistry of the latter. For this purpose we chose four phosphines, PMe_3 , PMe_2Ph , PEt_3 , and PEt_2Ph , and used two rather different solvents, namely, ethanol and benzene. Six of the products obtained have been characterized by X-ray crystallography, and also by mass spectroscopy and electrochemical measurements. Scheme 1 shows all the possible products, and their isomers, of the reactions with which we are concerned in this paper.

2. Experimental

2.1. General procedures

All the syntheses and purifications were carried out under an atmosphere of N_2 in standard Schlenkware. All solvents were freshly distilled under N_2 from suitable drying agents. The starting materials, $[\text{Bu}_4\text{N}]_2[\text{Re}_2\text{Cl}_8]$ (Aldrich); PMe_3 , PMe_2Ph , PEt_3 and PEt_2Ph (Strem Chemicals); and HI (0.75–1.00 M in CHCl_3) (Alfa Aesar) were used as received.



2.2. Physical measurements

Electrochemical measurements were carried out on dichloromethane solutions that contained 0.1 M tetra-*n*-butylammonium hexafluorophosphate (TBAH) as the supporting electrolyte. A stream of nitrogen was bubbled through the solution during the measurements. $E_{1/2}$ values, determined as $(E_{p,a} + E_{p,c})/2$, were referenced to the Ag/AgCl electrode at room temperature. Under our experimental conditions, $E_{1/2} = +0.47$ V versus Ag/AgCl for the ferrocenium/ferrocene couple. Voltammetric experiments were done with the use of a Bioanalytical Systems Inc. electrochemical analyzer, Model 100. The scan rate was 100 mV s^{-1} at a Pt disk electrode. The positive and negative FAB/DIP mass spectra were acquired using a VG Analytical 70S high-resolution, double-focusing, sector (EB) mass spectrometer. Samples for analyses were prepared by mixing a solution of each compound in CH_2Cl_2 or CHCl_3 with an NBA matrix on the direct insertion probe tip.

2.3. Syntheses

2.3.1. Preparation of $[\text{Bu}_4\text{N}]_2[\text{Re}_2\text{I}_8]$

The starting material, $[\text{Bu}_4\text{N}]_2[\text{Re}_2\text{I}_8]$, was prepared according to the published procedure [6]. An excess of HI (19 ml, 0.75–1.00 M solution in CHCl_3) was added to a suspension of $[\text{Bu}_4\text{N}]_2[\text{Re}_2\text{Cl}_8]$ (0.230 g, 0.2 mmol) in 8 ml of CH_2Cl_2 . The color of the mixture turned brown-black immediately. This was stirred for 4 h at room temperature (r.t.) without any further noticeable change. An excess of isomeric hexanes (120 ml) was then added to the mixture and it was kept at -10°C overnight to yield a black-purple crystalline precipitate. The product was collected by filtration; it was washed with hexanes until the washings were almost colorless, and dried. Yield: 0.307 g (78.2%).

Note: Both an excess of HI during the reaction and the extensive washing of the product with hexanes are crucial for the preparation of the octaiododirhenate. Otherwise, chloride-containing products such as $[\text{Re}_2\text{Cl}_4(\text{PMe}_3)_4]\text{I}$ may be obtained later.¹

¹ Crystal data for $[\text{Re}_2\text{Cl}_4(\text{PMe}_3)_4]\text{I} \cdot \text{CH}_2\text{Cl}_2$; brown-green crystal, $0.12 \text{ mm} \times 0.09 \text{ mm} \times 0.05 \text{ mm}$, $\text{Re}_2\text{P}_4\text{Cl}_6\text{I}_1\text{C}_{13}\text{H}_{38}$, orthorhombic space group $Pnma$ (No. 62), $a = 17.193(3)$, $b = 13.686(2)$, $c = 13.562(1)$ Å, $V = 3191.2(8)$ Å³, $Z = 4$, $T = -60^\circ\text{C}$. A total of 13 231 independent reflections were measured with $4.74 \leq 2\theta \leq 45.26^\circ$; 2219 independent reflections of which 1969 were observed [$I \geq 2\sigma(I)$]. Final full-matrix least-squares refinement on F^2 converged to $R_1 = 0.0390$, $wR_2 = 0.0781$ for all data, and $R_1 = 0.0329$, $wR_2 = 0.0734$ for data with $I \geq 2\sigma(I)$, GOF = 1.141. Re–Re = 2.2122(7) Å. See Section 4 for other structure details.

2.3.2. Reaction of $[Bu_4^nN]_2[Re_2I_8]$ with PMe_3 in ethanol to give $Re_2I_4(PMe_3)_4$ (**1a**)

PMe_3 (0.8 ml) was added to a suspension containing $[Bu_4^nN]_2[Re_2I_8]$ (0.196 g, 0.10 mmol) in 15 ml of ethanol. The reaction mixture, which turned dark brown immediately, was stirred at r.t. for 3 h. During this time a dark green solid precipitated. The mixture was reduced to half of its original volume and was then filtered. A dark green solid was isolated and washed with ethanol (2×10 ml), dried and then dissolved in 10 ml of dichloromethane. The dichloromethane solution was layered with 18 ml of isomeric hexanes at r.t. Dark green crystals of **1a**· CH_2Cl_2 appeared in one day. Yield: 0.080 g (65.1%). CV (CH_2Cl_2 , 22°C, V versus Ag/AgCl): $E_{1/2}(ox)(1) = -0.02$, $E_{1/2}(ox)(2) = +0.98$. FAB/DIP (NBA/ CH_2Cl_2 , m/z): 1184 ($[M]^+$), 1107 ($[M - PMe_3]^+$), 1031 ($[M - 2PMe_3]^+$), 904 ($[M - I - 2PMe_3]^+$), 803 ($[M - 3I]^+$).

2.3.3. Reaction of $[Bu_4^nN]_2[Re_2I_8]$ with PMe_2Ph in ethanol to give $Re_2I_4(PMe_2Ph)_4$ (**2a**)

PMe_2Ph (0.5 ml) was added to a suspension containing $[Bu_4^nN]_2[Re_2I_8]$ (0.411 g, 0.22 mmol) in 15 ml of ethanol. The mixture was stirred at r.t. for 1 h. During this time a green-brown solid precipitated. It was isolated by filtration, washed with hexanes (3×10 ml), dried, and dissolved in 15 ml of dichloromethane. The dichloromethane solution was layered with 20 ml of hexanes at r.t. Green crystals of **2a** started to grow in a few hours and the tube was left for a week. Yield: 0.201 g (63.8%). CV (CH_2Cl_2 , 22°C, V versus Ag/AgCl): $E_{1/2}(ox)(1) = -0.01$, $E_{1/2}(ox)(2) = +0.94$. FAB/DIP (NBA/ CH_2Cl_2 , m/z): 1433 ($[M]^+$), 1293 ($[M - PMe_2Ph]^+$), 1154 ($[M - 2PMe_2Ph]^+$), 1028 ($[M - I - 2PMe_2Ph]^+$), 899 ($[M - 2I - 2PMe_2Ph]^+$).

2.3.4. Reaction of $[Bu_4^nN]_2[Re_2I_8]$ with PEt_3 in ethanol to give $Re_2I_4(PEt_3)_4$ (**3a**)

PEt_3 (0.7 ml) was added to a suspension containing $[Bu_4^nN]_2[Re_2I_8]$ (0.215 g, 0.11 mmol) in 15 ml of ethanol at r.t. The reaction mixture turned brown immediately. It was stirred for 4 h at r.t. to give a brown precipitate. The solid was filtered, washed with hexanes and kept under vacuum for 18 h. It was then dissolved in 4 ml of dichloromethane, and the solution was layered with 11 ml of hexanes. Microcrystalline product **3a** appeared in a day. Yield: 0.082 g (55.2%). CV (CH_2Cl_2 , 22°C, V versus Ag/AgCl): $E_{1/2}(ox)(1) = -0.27$, $E_{1/2}(ox)(2) = +0.77$. FAB/DIP (NBA/ CH_2Cl_2 , m/z): 1352 ($[M]^+$), 1233 ($[M - PEt_3]^+$), 1118 ($[M - 2PEt_3]^+$), 980 ($[M - 2I - 2PEt_3]^+$).

2.3.5. Reaction of $[Bu_4^nN]_2[Re_2I_8]$ with PMe_3 in benzene to give $Re_2I_6(PMe_3)_4$ (**1b**)

PMe_3 (0.7 ml) was added to a suspension containing $[Bu_4^nN]_2[Re_2I_8]$ (0.196 g, 0.10 mmol) in 10 ml of benzene

at $\sim 10^\circ C$. The color of the reaction mixture turned black-purple immediately. It was stirred for 40 min, keeping the temperature at $\sim 10^\circ C$, and after that the mixture was filtered. The dark brown filtrate was evaporated to dryness, leaving a dark red-brown solid. Yield: 0.103 g (68.2%). Black-red crystals of **1b**· $2C_6H_6$ were obtained from the benzene solution (9 ml) layered with 17 ml of hexanes at r.t. in a few days. FAB/DIP (NBA/ CH_2Cl_2 , m/z): 1437 ($[M]^+$), 720 ($[M - Re - 3I - 2PMe_3]^+$), 593 ($[M - Re - 4I - 2PMe_3]^+$).

2.3.6. Reaction of $[Bu_4^nN]_2[Re_2I_8]$ with PMe_2Ph in benzene to give $Re_2I_4(PMe_2Ph)_4$ (**2a**)

PMe_2Ph (0.3 ml) was added to a suspension containing $[Bu_4^nN]_2[Re_2I_8]$ (0.111 g, 0.06 mmol) in 10 ml of benzene at $5-10^\circ C$. The mixture was stirred at that temperature for 1 h. During this time a green-brown solid precipitated. It was isolated by filtration, washed with hexanes (3×10 ml), dried, and dissolved in 10 ml of dichloromethane. The dichloromethane solution was layered with 20 ml of hexanes at r.t. Green crystals were grown over a few days. Yield: 0.037 g (43%). It was identified as complex **2a** by CV measurements and by X-ray diffraction.

2.3.7. Reaction of $[Bu_4^nN]_2[Re_2I_8]$ with PEt_3 in benzene to give $[Bu_4^nN][Re_2I_6(PEt_3)_2]$ (**3c**)

PEt_3 (0.7 ml) was added to a suspension containing $[Bu_4^nN]_2[Re_2I_8]$ (0.196 g, 0.10 mmol) in 14 ml of benzene. After stirring for 1 h at r.t., the reaction mixture turned purple and a solid was formed. The mixture was filtered and the filtrate was evaporated to dryness to give a purple solid. It was dried, washed with hexanes, and then dissolved in 8 ml of benzene. The purple benzene solution was layered with 20 ml of hexanes at r.t. to give dark green crystals of **3c**·(1/3) C_6H_6 in a week along with some unidentified solid. Yield: 0.059 g (36%).

2.3.8. Reaction of $[Bu_4^nN]_2[Re_2I_8]$ with PEt_2Ph in benzene to give $Re_2I_4(PEt_2Ph)_4$ (**4a**)

PEt_2Ph (0.6 ml) was added to a suspension containing $[Bu_4^nN]_2[Re_2I_8]$ (0.12 g, 0.06 mmol) in 12 ml of benzene at $5-10^\circ C$. The mixture turned dark purple immediately. It was stirred for 30 min, and then all volatiles were removed under reduced pressure to give an oily residue. This was washed with hexanes (3×10 ml), dried, and then dissolved in 10 ml of dichloromethane. The dichloromethane solution was layered with 18 ml of hexanes. Brown crystals of **4a** appeared over a period of five days. Yield: 0.054 g (55.8%). FAB/DIP (NBA/ CH_2Cl_2 , m/z): 1286 ($[M]^+$), 1120 ($[M - PEt_2Ph]^+$), 1032 ($[M - 2I]^+$), 905 ($[M - 3I]^+$).

Table 1

Crystallographic data for 1,3,6,8-Re₂I₄(PMe₃)₄·CH₂Cl₂ (**1a**·CH₂Cl₂), Re₂(μ-I)₂I₄(PMe₃)₄·2C₆H₆ (**1b**·2C₆H₆), 1,3,6-Re₂I₅(PMe₃)₃ (**1d**), 1,3,6,8-Re₂I₄(PMe₂Ph)₄ (**2a**), [Bu₄N][Re₂I₆(PEt₃)₂](1/3)C₆H₆ (**3c**·(1/3)C₆H₆), and 1,3,6,8-Re₂I₄(PMe₂Ph)₄ (**4a**)

	1a ·CH ₂ Cl ₂	1b ·2C ₆ H ₆	1d	2a	3c ·(1/3)C ₆ H ₆	4a
Formula	Re ₂ P ₄ I ₄ Cl ₂ C ₁₃ H ₃₈	Re ₂ P ₄ I ₆ C ₂₄ H ₄₈	Re ₂ P ₃ I ₅ C ₉ H ₂₇	Re ₂ P ₄ I ₄ C ₃₂ H ₄₄	Re ₂ P ₂ I ₆ N ₁ C ₃₀ H ₆₈	Re ₂ P ₄ I ₄ C ₄₀ H ₆₀
Crystal system	tetragonal	monoclinic	orthorhombic	orthorhombic	monoclinic	orthorhombic
Space group	I4 ₁ /acd (No. 142)	P2 ₁ /c (No. 14)	P2 ₁ 2 ₁ 2 ₁ (No. 19)	Fdd2 (No. 43)	C2/c (No. 15)	Pbca (No. 61)
Unit cell dimensions						
<i>a</i> (Å)	14.1714(4)	11.720(1)	9.742(1)	18.149(5)	38.970(2)	16.347(2)
<i>b</i> (Å)		16.251(4)	16.003(2)	45.47(2)	14.378(1)	23.212(2)
<i>c</i> (Å)	30.813(1)	11.490(2)	16.438(2)	9.423(2)	25.990(1)	24.495(3)
β (°)		104.17(3)			104.534(8)	
<i>V</i> (Å ³)	6188.1(3)	2121.8(7)	2562.7(5)	7776(4)	14097(1)	9295(2)
<i>Z</i>	8	2	4	8	12	8
Crystal size (mm)	0.15 × 0.12 × 0.10	0.20 × 0.18 × 0.15	0.25 × 0.15 × 0.13	0.18 × 0.12 × 0.08	0.18 × 0.12 × 0.10	0.30 × 0.20 × 0.10
Temperature (°C)	−60	−60	−60	−60	−60	−60
2θ Range (°)	4.84–45.00	5.10–45.04	4.86–44.96	4.96–45.08	4.24–45.02	4.52–45.10
Data/unique/observ.	15413/1013/966	9153/2769/2624	12171/3296/3221	7534/2480/2448	28413/8942/7072	38841/6038/5357
Restraints/parameters	0/60	0/133	42/159	1/191	41/520	1/458
<i>R</i> ₁ ^a , <i>wR</i> ₂ ^b [<i>I</i> > 2σ(<i>I</i>)]	0.0273, 0.0618	0.0272, 0.0723	0.0599, 0.1480	0.0275, 0.0723	0.0550, 0.1137	0.0424, 0.0997
<i>R</i> ₁ ^a , <i>wR</i> ₂ ^b (all data)	0.0285, 0.0626	0.0294, 0.0753	0.0612, 0.1496	0.0279, 0.0728	0.0773, 0.1302	0.0504, 0.1117
Goodness-of-fit ^c	1.207	1.118	1.041	1.084	1.102	1.123

^a $R_1 = \sum ||F_o| - |F_c|| / \sum |F_o|$.

^b $wR_2 = [\sum [w(F_o^2 - F_c^2)^2] / \sum [w(F_o^2)^2]]^{1/2}$.

^c Goodness-of-fit = $[\sum [w(F_o^2 - F_c^2)^2] / (N_{\text{observns}} - N_{\text{params}})]^{1/2}$, based on all data.

2.3.9. Reaction of Re₂I₆(PMe₃)₄ with KC₈ to give **1a** and Re₂I₅(PMe₃)₃ (**1d**)

The solid Re₂I₆(PMe₃)₄ (0.100 g, 0.07 mmol) was mixed with a twofold excess of KC₈ (made according to the literature procedure [7]). Then 10 ml of toluene was added to the mixture followed by 5 ml of CH₂Cl₂. The mixture was stirred at 0°C for 1 h, and filtered after that. The brown filtrate was layered with 18 ml of hexanes. After the layers were mixed the volume was reduced by half. Next day dark green crystals of **1a** appeared on the walls of the tube, along with a few brown crystals of **1d**.

2.4. X-ray structure determinations

Single crystals of compounds **1a**·CH₂Cl₂, **1b**·2C₆H₆, **1d**, **2a**, **3c**·(1/3)C₆H₆, and **4a** were obtained as described above. All X-ray diffraction experiments were carried out on a Nonius FAST diffractometer with an area detector using Mo Kα radiation ($\lambda = 0.71073$ Å). Details concerning the data collection have been fully described elsewhere [8]. Each crystal was mounted on the tip of a quartz fiber with silicone grease, and the setup was quickly placed in the cold N₂ stream (−60°C) of a Model FR 558-S low-temperature controller. Fifty reflections were used in cell indexing and about 250 reflections in cell refinement. Axial images were obtained to confirm the Laue group and cell dimensions. The data were corrected for Lorentz and

polarization effects by the MADNES program [9]. Reflection profiles were fitted and values of F^2 and $\sigma(F^2)$ for each reflection were obtained by the program PROCOR [10].

All calculations were carried out on a DEC Alpha running VMS. The structures were solved and refined using the SHELXTL direct methods [11] and the SHELXL-93 programs [12]. In all structures hydrogen atoms were included in the structure factor calculations at idealized positions. All crystals of **2a** appeared to be racemic twins; therefore twin refinement was used (BASF = 0.66). There was a complication in the structure of **3c**·(1/3) C₆H₆ due to the observation of three-way disorder (85.7:9.9:4.4 and 82.4:13.2:4.4% for two crystallographically independent anions, respectively) of the dirhenium units (often encountered with in the species of the type Re₂X₆P₂ [1]) along with severe disorder of the tetrabutylammonium cations and benzene solvation molecules. A second orientation of the Re₂ (1.25%) was also introduced in the refinement of **4a**. The dirhenium unit was also found to be disordered over three orientations (91.7:6.4:1.9%) in the crystal of **1d**. Two sets of ligands (I and PMe₃) were modeled and refined with equal occupancies in this experiment. The relevant crystallographic data for complexes **1a**·CH₂Cl₂, **1b**·2C₆H₆, **1d**, **2a**, **3c**·(1/3)C₆H₆, and **4a** are summarized in Table 1. An X-ray experiment was also carried out for a side-product [1,3,6,8-Re₂Cl₄(PMe₃)₄][I·CH₂Cl₂].¹ These data can be found in Section 4.

3. Results and discussion

3.1. Syntheses

While it was observed a long time ago [2] that reactions of $[\text{Re}_2\text{I}_8]^{2-}$ with monodentate phosphines in ethanol or acetone media lead to the two-electron reduction products $\text{Re}_2\text{I}_4(\text{PR}_3)_4$ ($\text{R} = \text{Et}, \text{Pr}^n, \text{Bu}^n$) within a few minutes at room temperature, the structures of these mixed phosphine/iodide compounds have never been determined. They were assumed to be the 1,3,6,8 isomers, the only type known at that time. In contrast to this, prolonged reflux is needed to convert the analogous $[\text{Re}_2\text{Cl}_8]^{2-}$ to the $\text{Re}_2\text{Cl}_4(\text{PR}_3)_4$ compounds. The reactions of $[\text{Re}_2\text{Cl}_8]^{2-}$ with the most basic monodentate phosphines, PMe_3 and PMe_2Ph , also proceed at room temperature in ethanol; they require hours to reach the stage of one-electron reduction products, namely the 1,2,7-isomers of $\text{Re}_2\text{Cl}_5(\text{PR}_3)_3$ [5b,13]. These complexes, which have two phosphine ligands located *cis* to each other on one rhenium atom (Scheme 1) have been used recently [5a,b] as starting materials to prepare a new class of 1,2,7,8 isomers of the $\text{Re}_2\text{Cl}_4(\text{PR}_3)_4$ stoichiometry.

These findings on the existence of a previously unknown *cis* type of geometry for the $\text{Re}_2\text{Cl}_4(\text{PR}_3)_4$ stoichiometry gave us an incentive to reinvestigate the 'old' processes involving $[\text{Re}_2\text{I}_8]^{2-}$. Since transformations of octaiododirhenate into the $\text{Re}_2\text{I}_4\text{P}_4$ core compounds proceed under very mild conditions (room temperature and short reaction times) it was considered possible that *cis* type products might form directly with sterically undemanding ligands. Therefore we choose two small cone-angle phosphines, PMe_3 and PMe_2Ph , which were not studied in reactions with $[\text{Re}_2\text{I}_8]^{2-}$ before

[2,3], but were shown in the dirhenium chloride chemistry to afford a number of products with a *cis* location of ligands at the rhenium atoms. We expected that the most basic phosphines, PMe_3 and PMe_2Ph , would as readily afford $\text{Re}_2\text{I}_4(\text{PR}_3)_4$ products in ethanol as the more bulky and less basic ones (PEt_3 , PPr_3^n , PBu_3^n) examined previously [2].

We first performed the reactions of $[\text{Re}_2\text{I}_8]^{2-}$ with sterically undemanding ligands, PMe_3 and PMe_2Ph , in ethanol so as to isolate the reduced products of the Re_2^{4+} core in crystalline form and to confirm their stereochemistry by an X-ray diffraction study. Second, we used benzene as a medium for the reactions of $[\text{Re}_2\text{I}_8]^{2-}$ with a number of different monodentate phosphines, PMe_3 , PMe_2Ph , PEt_3 and PEt_2Ph , since benzene was earlier shown to be a solvent that allows isolation of some intermediates and/or kinetic products in the mixed chloride/phosphine dirhenium chemistry [5]. The key difference between the two solvents is that ethanol has the potential to be a reducing agent whereas benzene does not. We note again that stoichiometries different from the $\text{Re}_2\text{I}_4(\text{PR}_3)_4$ have not been seen in any previously studied reactions involving $[\text{Re}_2\text{I}_8]^{2-}$ [1–3].

For reactions between $[\text{Re}_2\text{I}_8]^{2-}$ and PMe_3 and PMe_2Ph in ethanol we confirmed the observations made before [2] that complete transformation of the $[\text{Re}_2\text{I}_8]^{2-}$ in alcohol takes place within minutes at room temperature in the presence of monodentate phosphines to give the Re_2^{4+} products, $\text{Re}_2\text{I}_4(\text{PR}_3)_4$ ($\text{R}_3 = \text{Me}_3$ (**1a**) and Me_2Ph (**2a**)) in good yield. The cyclic voltammograms exhibited two reversible oxidations, which is consistent with the data published before (Table 2), and the molecular structures in the solid state revealed a *trans* geometry of the phosphine ligands for both compounds (vide supra).

Having found that such small-cone angle phosphine ligands as PMe_3 and PMe_2Ph afforded only *trans* products in the iodide case, we then switched to benzene. The use of benzene as a solvent for the reactions of $[\text{Re}_2\text{I}_8]^{2-}$ with phosphine ligands allowed us, as expected, to slow down the transformation and to isolate some intermediate iodide products, much as in the case of the analogous reactions involving $[\text{Re}_2\text{Cl}_8]^{2-}$ [5]. The use of benzene afforded novel stoichiometries for the mixed iodide/phosphine complexes that had not been observed before. Thus, the reaction of $[\text{Re}_2\text{I}_8]^{2-}$ with PMe_3 in benzene for 30 min afforded a new dirhenium-(III) iodide complex, $\text{Re}_2\text{I}_6(\text{PMe}_3)_4$ (**1b**). It is a kinetic product of the reaction, which is controlled by temperature, time, ratio of reagents, etc. The best yields of **1b** were observed when the reaction was performed at about 10°C under conditions described in Section 2.3.5. At room temperature the thermodynamic product **1a** was formed in a mixture with **1b** due to a type of disproportionation mechanism discovered recently [5e].

Table 2
Voltammetric $E_{1/2}$ values (V) for the mixed phosphine/halide dirhenium(II,II) compounds, 1,3,6,8- $\text{Re}_2\text{X}_4(\text{PR}_3)_4$

X	$E_{1/2}(\text{ox})(1)$	$E_{1/2}(\text{ox})(2)$	Ref.
PMe₃			
Cl	−0.23	+0.96	[14]
Br	−0.11	+1.01	[14]
I	−0.02	+0.98	this work
PMe₂Ph			
Cl	−0.30	+0.83	[3]
I	−0.01	+0.94	this work
PEt₃			
Cl	−0.42	+0.80	[3]
Br	−0.31	+0.83	[3]
I	−0.27	+0.77	[3], this work
PPr₃			
Cl	−0.44	+0.79	[3]
Br	−0.38	+0.84	[3]
I	−0.22	+0.85	[3]

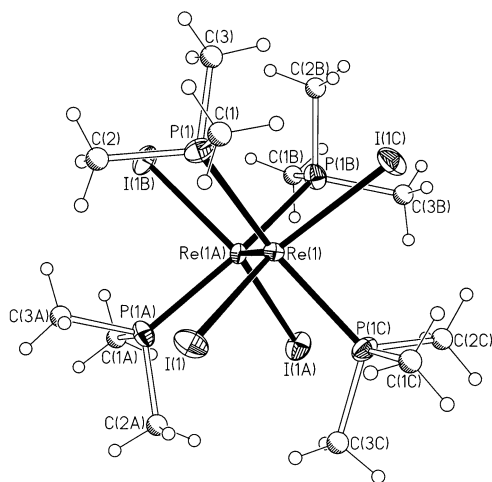


Fig. 1. A perspective drawing of 1,3,6,8- $\text{Re}_2\text{I}_4(\text{PMe}_3)_4$ (**1a**). Atoms are represented by thermal ellipsoids at the 40% probability level. Carbon and hydrogen atoms are shown as spheres of arbitrary radii.

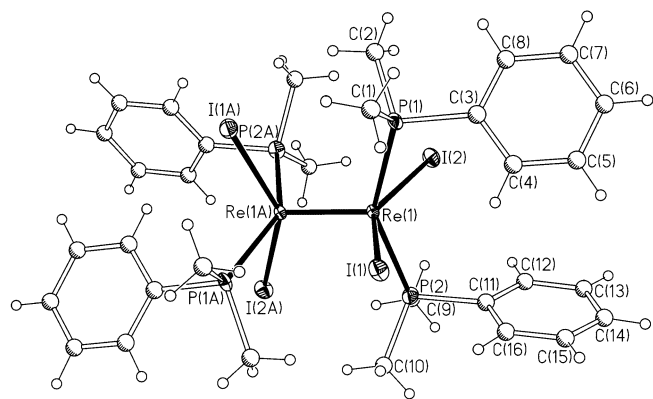


Fig. 2. A perspective drawing of 1,3,6,8- $\text{Re}_2\text{I}_4(\text{PMe}_2\text{Ph})_4$ (**2a**). Atoms are represented by thermal ellipsoids at the 40% probability level. Carbon and hydrogen atoms are shown as spheres of arbitrary radii.

From the reaction of $[\text{Re}_2\text{I}_8]^{2-}$ with PET_3 in benzene at room temperature we isolated another kinetic product, namely $[\text{Bu}_4\text{N}][\text{Re}_2\text{I}_6(\text{PET}_3)_2]$ (**3c**). It is the first iodide complex of $\text{Re}_2\text{I}_6\text{P}_2$ stoichiometry, although it was crystallized in its monoanionic form as in the analogous reaction of $[\text{Re}_2\text{Cl}_8]^{2-}$ [5e]. We believe that this is just one of the kinetic intermediates formed in this system as CV measurements of reaction products in the system $[\text{Re}_2\text{I}_8]^{2-}/\text{PET}_3$ showed the presence of other intermediates. In addition, the formation of the oxidized product, $\text{ReI}_4(\text{PET}_3)_2$, in the system was observed by mass spectroscopy. We were unable to get these compounds in the crystalline form, but nevertheless they support the disproportionation mechanism of transformations in benzene, $3\text{Re}_2^{6+} \rightarrow 2\text{Re}_2^{5+} + 2\text{Re}^{4+}$, as previously observed in the reactions of $[\text{Re}_2\text{Cl}_8]^{2-}$ [5e].

In contrast to the above-mentioned reactions, the reactions of $[\text{Re}_2\text{I}_8]^{2-}$ with PMe_2Ph and PET_2Ph in benzene yield only complexes of the Re_2^{4+} core, **2a**, and

its analog $\text{Re}_2\text{I}_4(\text{PET}_2\text{Ph})_4$ (**4a**), at least in our hands. In this case the transformation probably proceeds so fast even at 5°C that we were unable to isolate any intermediates. In general, we found that reactions for octaiododirhenium in benzene proceed much faster than for $[\text{Re}_2\text{Cl}_8]^{2-}$ and afford a mixture of products with quite low yields. Nevertheless, we were able to observe some new stoichiometries, previously unknown for the rhenium iodides. We also used product **1b** of the Re_2^{6+} core as a starting material for reduction by KC_8 and this reaction yielded the formation of **1a** and a few crystals of the new Re_2^{5+} core compound, $\text{Re}_2\text{I}_5(\text{PMe}_3)_3$ (**1d**), as a result of incomplete reduction.

3.2. Electrochemical data

It is known [1] that the derivatives of dirhenium(II) $\text{Re}_2\text{X}_4\text{P}_4$ exhibit a redox chemistry that is both interesting and extensive. Some electrochemical data for the mixed phosphine/halide complexes of the type 1,3,6,8- $\text{Re}_2\text{X}_4(\text{PR}_3)_4$ have been already reported [2,3], and now we extend these series by adding two more iodide complexes of this type for $\text{PR}_3 = \text{PMe}_3$ and PMe_2Ph (Table 2). All the complexes behave in a similar fashion: the cyclic voltammograms show two electrochemically reversible, one-electron oxidation waves corresponding to two oxidation reactions $[\text{Re}_2\text{X}_4(\text{PR}_3)_4]/[\text{Re}_2\text{X}_4(\text{PR}_3)_4]^+$ and $[\text{Re}_2\text{X}_4(\text{PR}_3)_4]^+/[\text{Re}_2\text{X}_4(\text{PR}_3)_4]^{2+}$. There is an interesting and clear trend, namely $E_{1/2}(\text{ox})(1)$ for iodides $> E_{1/2}(\text{ox})(1)$ for the corresponding chlorides, with bromides being an intermediate case, while the $E_{1/2}(\text{ox})(2)$ values for the reported halides are close. This implies indirectly that the second reduction to $\text{Re}_2\text{X}_4(\text{PR}_3)_4$ complexes from $[\text{Re}_2\text{X}_4(\text{PR}_3)_4]^+$ cations, which we found to be a limiting stage in the analogous chloride system [5d], goes more easily for iodides and can be achieved at room temperature.

3.3. Crystal structures

Since there was no crystal structure of any dirhenium iodide other than $[\text{Re}_2\text{I}_8]^{2-}$ itself [6b] reported before, it is interesting to compare those now available with the structures of the corresponding chlorides so as to determine the effect of the bulky iodine atoms upon the overall geometries of the molecules. For two phosphines, PMe_3 and PMe_2Ph , from reactions in ethanol we isolated $\text{Re}_2\text{I}_4(\text{PR}_3)_4$ ($\text{R}_3 = \text{Me}_3$ (**1a**) and Me_2Ph (**2a**)). One more complex of the same stoichiometry was obtained from benzene, $\text{Re}_2\text{I}_4(\text{PET}_2\text{Ph})_4$ (**4a**). For all of them the X-ray diffraction study revealed the 1,3,6,8 type of stereochemistry (Figs. 1–3) with *trans* phosphine ligands on both the rhenium atoms. There are corresponding chloride analogs for **1a** [15] and **2a** [16], but not for **4a**. The Re–Re distances in **1a** and **2a**

(Table 3) are not significantly different, namely 2.2541(8) and 2.258(1) Å, while the Re–Re separation in **4a** is a bit longer, 2.2698(7) Å, but all of them are

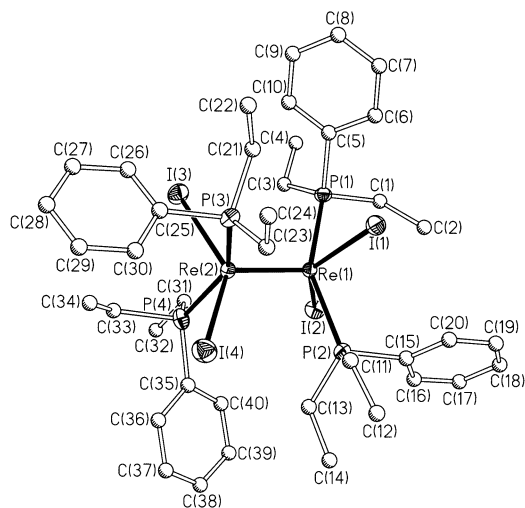


Fig. 3. A perspective drawing of 1,3,6,8- $\text{Re}_2\text{I}_4(\text{PEt}_2\text{Ph})_4$ (**4a**). Atoms are represented by thermal ellipsoids at the 40% probability level. Carbon atoms are shown as spheres of an arbitrary radius. Hydrogen atoms of the ethyl and phenyl groups are omitted for clarity.

Table 3

Selected mean bond distances (Å), angles (°) and torsion angles (°) for $\text{Re}_2\text{I}_4(\text{PR}_3)_4$ ($\text{R}_3 = \text{Me}_3$ (**1a**), Me_2Ph (**2a**), and Et_2Ph (**4a**))

	1a	2a	4a
<i>Bond distances</i>			
Re–Re	2.2541(8)	2.258(1)	2.2698(7)
Re–P	2.427(2)	2.453(3)	2.475(3)
Re–I	2.7108(5)	2.7157(9)	2.6969(9)
<i>Bond angles</i>			
P–Re–P	155.0(1)	146.39(9)	149.7(1)
P–Re–I	84.90(5)	85.08(7)	84.51(7)
I–Re–I	131.36(3)	145.23(3)	136.96(3)
Re–Re–I	114.32(2)	107.36(2)	111.52(3)
Re–Re–P	102.48(5)	106.80(7)	105.15(7)
P–Re–Re–I	0	11.95(8)	6.92(8)

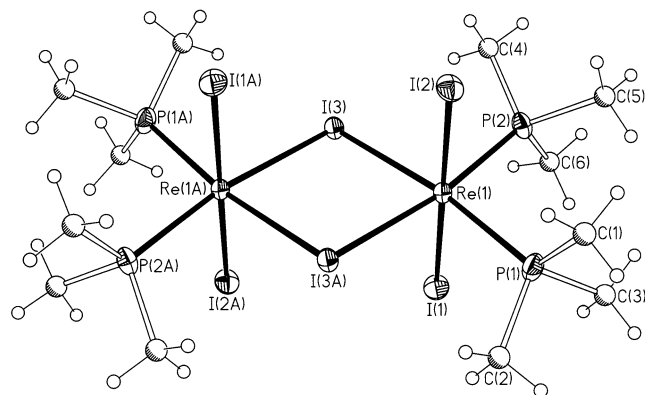


Fig. 4. A perspective drawing of $\text{Re}_2(\mu\text{-I})_2\text{I}_4(\text{PMe}_3)_4$ (**1b**). Atoms are represented by thermal ellipsoids at the 40% probability level. Carbon and hydrogen atoms are shown as spheres of arbitrary radii.

Table 4

Selected bond distances (Å) and angles (deg) for $\text{Re}_2(\mu\text{-I})_2\text{I}_4(\text{PMe}_3)_4$ (**1b**) and $\text{Re}_2(\mu\text{-Cl})_2\text{Cl}_4(\text{PMe}_3)_4$

	1b X = I	$\text{Re}_2(\mu\text{-Cl})_2\text{Cl}_4(\text{PMe}_3)_4$ ^a X = Cl
<i>Bond distances</i>		
Re(1)···Re(1A)	4.274(1)	3.8476(4)
Re–P	2.403(2)	2.375(1)
Re–X _t ^b	2.680(1)	2.341(1)
Re–X _{br} ^c	2.8130(7)	2.512(1)
<i>Bond angles</i>		
P–Re–P	95.08(7)	93.91(5)
X _t –Re–X _t	179.00(2)	178.60(5)
X _{br} –Re–X _{br}	81.12(2)	80.02(4)
P–Re–X _t	85.96(6)–94.26(5)	86.57(5)–93.36(4)
P–Re–X _{br}	92.05(5), 171.87(5)	92.85(4), 172.01(4)
X _t –Re–X _{br}	89.32(2)–91.33(2)	89.65(4)–90.78(4)
Re–X _{br} –Re	98.88(2)	99.98(4)

^a From Ref. [5a].

^b X_t — terminal halide atom.

^c X_{br} — bridging halide atom.

appropriate for a rhenium–rhenium triple bond [1]. The only significant difference between the geometric characteristics of the corresponding chlorides and iodides is, naturally, the rhenium–halide distance, which is about 0.3 Å greater for the latter. All the angles Re–Re–L (L = P, X) are also similar. It may be noted that while the structure of **1a** is perfectly eclipsed, the molecules of **2a** and **4a** are partially staggered. The mean P–Re–Re–I angle for the PMe_2Ph compound (**2a**) of 12° is the highest for any known molecule of the $1,3,6,8\text{-Re}_2\text{X}_4(\text{PR}_3)_4$ isomer type. Interestingly, the corresponding angle in $1,3,6,8\text{-Re}_2\text{Cl}_4(\text{PMe}_2\text{Ph})_4$ is the highest among all the isotypical chlorides.

From the reaction of $[\text{Re}_2\text{I}_8]^{2-}$ with PMe_3 in benzene a complex of composition $\text{Re}_2\text{I}_6(\text{PMe}_3)_4$ (**1b**) was isolated, for which an X-ray structural analysis revealed an edge-sharing bioctahedral structure with all of the trimethylphosphine ligands in the same plane as the metal centers and the bridging iodide ions (Fig. 4). Complex **1b** is a centrosymmetric iodide-bridged dirhenium molecule analogous to the $1,3,5,7\text{-Re}_2(\mu\text{-Cl})_2\text{Cl}_4(\text{PMe}_3)_4$ [5a]. Although there was no reduction process in this case, the Re_2^{6+} core has been disrupted in this complex to give a very long Re···Re separation of 4.274(1) Å (Table 4). This is much greater than the value of 3.8476(4) Å in the analogous chloride due to the considerably larger size of the bridging iodine atoms. As expected, the Re–I_{br} distances of 2.8130(7) Å in **1b** are significantly greater, by 0.133 Å, than the Re–I_t of 2.680(1) Å. In general, the Re–I distances in **1b** are about 0.3 Å greater than those of the Re–Cl in the related chloride molecule, while the difference in the Re–P distances is less by an order of magnitude. The remaining characteristics, including the angles Re–I_{br}–Re, I_{br}–Re–I_{br}, and I_t–Re–I_t are very similar to

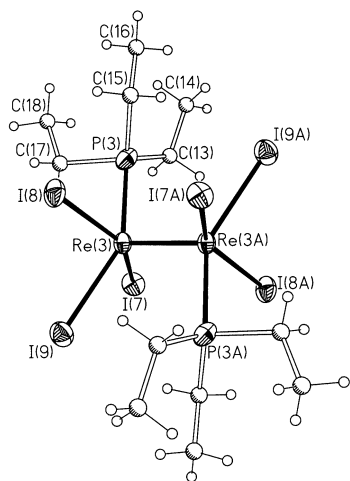


Fig. 5. A perspective drawing of one of the two crystallographically independent $[\text{Re}_2\text{I}_6(\text{PEt}_3)_2]^-$ anions from **3c**. Atoms are represented by thermal ellipsoids at the 30% probability level. Carbon and hydrogen atoms are shown as spheres of arbitrary radii. Only the major orientation of the disordered dirhenium unit and one orientation of the ethyl groups are depicted.

those of the chloride analog [5a]. It would seem certain that there is no $\text{Re}\cdots\text{Re}$ interaction in **1b** in view of the great metal–metal distance and the obtuse $\text{Re}-\text{I}_{\text{br}}-\text{Re}$ angle of $98.88(2)^\circ$ [17].

In the molecule of **1b** the PMe_3 ligands are located *cis* to each other on each $\text{Re}(\text{III})$ center with an angle $\text{P}(1)-\text{Re}-\text{P}(2)$ of $95.08(7)^\circ$. It is interesting to compare the characteristics of **1b** with the data for two other bioctahedral edge-sharing iodides of the same 1,3,5,7 structural type, namely $\text{Zr}_2(\mu-\text{I})_2\text{I}_4(\text{PMe}_3)_4$ [18] and $\text{Hf}_2(\mu-\text{I})_2\text{I}_4(\text{PMe}_3)_4$ [19]. In contrast to **1b**, the zirconium and hafnium iodide-bridged complexes were formulated, based on the structural, spectroscopic and theoretical data, as diamagnetic dimers with a substantial amount of metal–metal bonding. The degree of $\text{M}-\text{M}$ interaction for an M_2X_6 core has been in general corre-

Table 5

Selected mean bond distances (\AA) and angles ($^\circ$) for $[\text{Re}_2\text{I}_6(\text{PEt}_3)_2]^-$ in **3c**

Bond distances

$\text{Re}(1)-\text{Re}(2)$	2.233(1)			$\text{Re}(3)-\text{Re}(3')$	2.240(1)
$\text{Re}(1)-\text{P}(1)$	2.452(4)	$\text{Re}(2)-\text{P}(2)$	2.414(5)	$\text{Re}(3)-\text{P}(3)$	2.439(5)
$\text{Re}(1)-\text{I}(1)$	2.70(2)	$\text{Re}(2)-\text{I}(5)$	2.71(2)	$\text{Re}(3)-\text{I}(7)$	2.699(1)
$\text{Re}(1)-\text{I}(2)$	2.74(1)	$\text{Re}(2)-\text{I}(6)$	2.74(2)	$\text{Re}(3)-\text{I}(9)$	2.742(2)
$\text{Re}(1)-\text{I}(3)$	2.70(2)	$\text{Re}(2)-\text{I}(4)$	2.71(2)	$\text{Re}(3)-\text{I}(8)$	2.687(1)

Bond angles

$\text{P}(1)-\text{Re}(1)-\text{I}(1)$	84.3(3)	$\text{P}(2)-\text{Re}(2)-\text{I}(5)$	83.9(6)	$\text{P}(3)-\text{Re}(3)-\text{I}(7)$	86.2(1)
$\text{P}(1)-\text{Re}(1)-\text{I}(2)$	147.8(4)	$\text{P}(2)-\text{Re}(2)-\text{I}(6)$	144.7(5)	$\text{P}(3)-\text{Re}(3)-\text{I}(9)$	146.2(1)
$\text{P}(1)-\text{Re}(1)-\text{I}(3)$	88.3(3)	$\text{P}(2)-\text{Re}(2)-\text{I}(4)$	88.7(3)	$\text{P}(3)-\text{Re}(3)-\text{I}(8)$	86.5(1)
$\text{I}(1)-\text{Re}(1)-\text{I}(2)$	85.6(5)	$\text{I}(5)-\text{Re}(2)-\text{I}(6)$	84.8(6)	$\text{I}(7)-\text{Re}(3)-\text{I}(9)$	83.92(4)
$\text{I}(1)-\text{Re}(1)-\text{I}(3)$	146.3(6)	$\text{I}(4)-\text{Re}(2)-\text{I}(5)$	148.9(7)	$\text{I}(7)-\text{Re}(3)-\text{I}(8)$	147.81(5)
$\text{I}(2)-\text{Re}(1)-\text{I}(3)$	83.3(5)	$\text{I}(4)-\text{Re}(2)-\text{I}(6)$	84.3(5)	$\text{I}(8)-\text{Re}(3)-\text{I}(9)$	84.96(2)
$\text{Re}(2)-\text{Re}(1)-\text{P}(1)$	100.4(1)	$\text{Re}(1)-\text{Re}(2)-\text{P}(2)$	101.8(1)	$\text{Re}(3\text{A})-\text{Re}(3)-\text{P}(3)$	98.6(1)
$\text{Re}(2)-\text{Re}(1)-\text{I}(1)$	106.3(4)	$\text{Re}(1)-\text{Re}(2)-\text{I}(5)$	106.6(6)	$\text{Re}(3\text{A})-\text{Re}(3)-\text{I}(7)$	106.05(5)
$\text{Re}(2)-\text{Re}(1)-\text{I}(2)$	111.7(4)	$\text{Re}(1)-\text{Re}(2)-\text{I}(6)$	113.6(5)	$\text{Re}(3\text{A})-\text{Re}(3)-\text{I}(9)$	115.21(6)
$\text{Re}(2)-\text{Re}(1)-\text{I}(3)$	107.4(4)	$\text{Re}(1)-\text{Re}(2)-\text{I}(4)$	103.9(4)	$\text{Re}(3\text{A})-\text{Re}(3)-\text{I}(8)$	106.03(5)
$\text{P}(1)-\text{Re}(1)-\text{Re}(2)-\text{P}(2)$	165.9(2)			$\text{P}(3)-\text{Re}(3)-\text{Re}(3\text{A})-\text{P}(3\text{A})$	180.0

lated [17] to the $\text{M}-\text{M}$ distances and the angular parameters. The latter, namely the acute angles $\text{M}-\text{I}_{\text{br}}-\text{M}$ of $72.04(4)$ and $71.21(3)^\circ$ in the Zr and Hf compounds, respectively, contrasts with the value of $98.88(2)^\circ$ in **1b**. The metal–metal distances of $3.393(2)$ \AA in Zr and of $3.328(1)$ \AA in Hf analogs (which are considerably shorter than that in **1b**) have been assigned as long but real $\text{M}-\text{M}$ single bonds [18].

The reaction of $[\text{Re}_2\text{I}_8]^{2-}$ with PEt_3 in benzene at room temperature afforded a new kinetic product, $[\text{Bu}_4\text{N}][\text{Re}_2\text{I}_6(\text{PEt}_3)_2]$ (**3c**). The chloride analog has been obtained by us using the same approach, but the structural characterization was not satisfactory because of a severe disorder problem. The crystal structure of **3c** consists of paramagnetic dirhenium anions of the Re_2^{5+} core (Fig. 5) and tetrabutylammonium cations. There are two crystallographically distinct $[\text{Re}_2\text{I}_6(\text{PEt}_3)_2]^-$ units in the structure, only one of which has an inversion center at the midpoint of the $\text{Re}-\text{Re}$ bond. The centrosymmetric molecule is less disordered and fully eclipsed, while the noncentrosymmetric one is partially staggered with a $\text{P}-\text{Re}-\text{Re}-\text{P}$ torsion angle of 166° . Similar features have been also observed for analogous chlorides.

Two different isomeric forms of the $\text{Re}_2\text{Cl}_6\text{P}_2$ core (Scheme 1) have been recognized in the solid state by X-ray crystallography, including an unprecedented 1,6 rotamer with C_2 symmetry, which we discovered recently [5f]. Most structures of the $\text{Re}_2\text{Cl}_6\text{P}_2$ stoichiometry, both in the neutral and monoanionic forms, belong to the presumably more stable 1,7 isomer type with C_{2h} virtual symmetry. The dirhenium iodide/phosphine anions in **3c** also show the 1,7 disposition of the triethylphosphine ligands. The *trans* influence of the phosphine ligands is reflected in the fact that the $\text{Re}-\text{I}$ bonds (Table 5) *trans* to the P atoms are about 0.04 \AA longer than those *trans* to the I atoms. There is also a

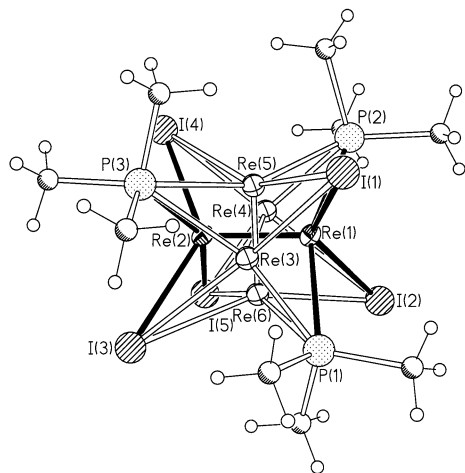


Fig. 6. A drawing showing the three orientations of the Re_2 unit for the 1,3,6,8- $\text{Re}_2\text{I}_5(\text{PMe}_3)_3$ (**1d**) molecule. Only one orientation of the ligands is presented. Carbon and hydrogen atoms are not labeled for clarity.

Table 6
Selected mean bond distances (Å) and angles (°) for 1,3,6,8- $\text{Re}_2\text{I}_5(\text{PMe}_3)_3$ (**1d**)

Bond distances			
Re(1)–Re(2)	2.235(1)		
Re(1)–P(1)	2.47(1)	Re(2)–P(3)	2.452(7)
Re(1)–P(2)	2.47(1)	Re(2)–I(3)	2.653(5)
Re(1)–I(1)	2.667(4)	Re(2)–I(4)	2.673(6)
Re(1)–I(2)	2.659(5)	Re(2)–I(5)	2.740(4)
Bond angles			
P(1)–Re(1)–P(2)	154.5(4)	P(3)–Re(2)–I(5)	155.5(2)
P(1)–Re(1)–I(1)	85.8(4)	P(3)–Re(2)–I(3)	83.8(2)
P(1)–Re(1)–I(2)	82.2(4)	P(3)–Re(2)–I(4)	83.5(2)
P(2)–Re(1)–I(1)	87.4(4)	I(3)–Re(2)–I(5)	86.8(2)
P(2)–Re(1)–I(2)	84.1(4)	I(4)–Re(2)–I(5)	87.6(2)
I(1)–Re(1)–I(2)	131.9(1)	I(3)–Re(2)–I(4)	135.3(2)

steric effect that causes the Re–Re–I angles for the iodine atoms facing the phosphorus ligands to be 10° greater than the others.

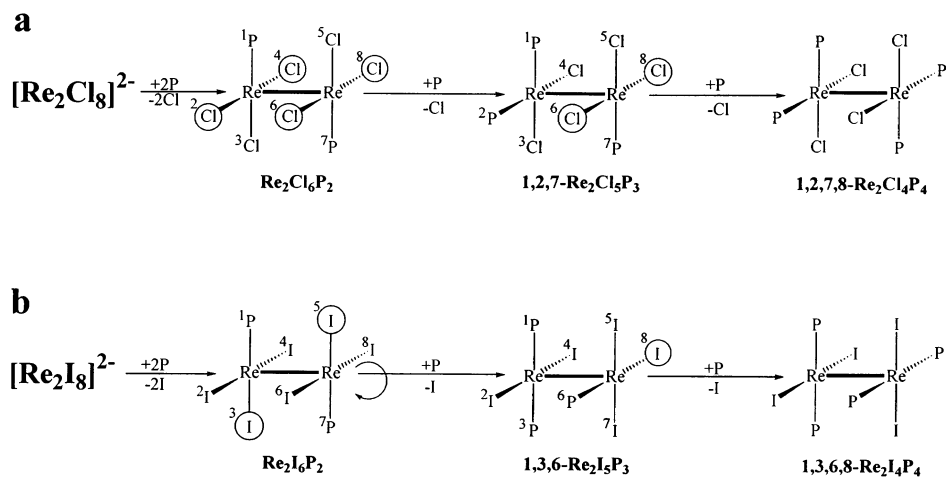
Another Re_2^{5+} core compound is represented by the 1,3,6-isomer of $\text{Re}_2\text{I}_5(\text{PMe}_3)_3$ (**1d**) having two phosphine ligands *trans* to each other on one of the rhenium atoms (the P–Re–P angle is $154.5(4)^\circ$). As is common for this type of structure, the molecule of **1d** is eclipsed and shows a three-way disorder of the dimetal unit. Note that for all three orientations we have the same 1,3,6-isomer (Fig. 6). The Re–Re distance of 2.235(1) Å (Table 6) is the same as for the chloride analogs [13b] and is typical for the bond order of 3.5. Again, we should mention the *trans* effect of the phosphine groups leading to the elongation of the Re–I (~ 0.08 Å) and the Re–P (~ 0.02 Å) bonds *trans* to the P atoms in relation to those which are *trans* to the I atoms.

3.4. Reactivity of $[\text{Re}_2\text{I}_8]^{2-}$ versus $[\text{Re}_2\text{Cl}_8]^{2-}$

The reactivity of $[\text{Re}_2\text{I}_8]^{2-}$ toward monodentate phosphine ligands in ethanol contrasts quite strikingly with that observed for the corresponding chloride, $[\text{Re}_2\text{Cl}_8]^{2-}$. All processes associated with the transformation of $[\text{Re}_2\text{I}_8]^{2-}$ in the presence of phosphines, namely, the substitution of I^- by PR_3 and the reduction of the Re_2^{6+} to the Re_2^{4+} core products, are significantly faster at room temperature for the iodide than for $[\text{Re}_2\text{Cl}_8]^{2-}$. In all cases the reduction of the $[\text{Re}_2\text{I}_8]^{2-}$ is practically complete in a few minutes. For the first time products of $\text{Re}_2\text{I}_4(\text{PR}_3)_4$ stoichiometry have been structurally characterized in this work for $\text{R}_3 = \text{Me}_3$ (**1a**), Me_2Ph (**2a**), and Et_2Ph (**4a**), and they are found to be 1,3,6,8 isomers. Formation of the *trans*, *trans* type of products even for the small cone-angle phosphines, PMe_3 and PMe_2Ph , lends credibility to the assignment of 1,3,6,8 geometry to the $\text{Re}_2\text{I}_4(\text{PR}_3)_4$ ($\text{R} = \text{Et}, \text{Pr}^n, \text{Bu}^n$) compounds made long ago by spectroscopic and electrochemical techniques [2,3]. Possible reasons why both substitution and reduction proceed faster for $[\text{Re}_2\text{I}_8]^{2-}$ could be the higher lability of the iodide compared to the chloride anion, and a general tendency of iodides to be more easily reduced than chlorides [20]. It is also possible that I^- , in addition to the alcohol, can assist in the reduction of the dirhenium unit by oxidation to the I_2 . It was not possible to speculate about the mechanism of these processes until some intermediate species were detected. The reactions in benzene are very important because they allow us to observe some kinetic products.

In general, the reactions of $[\text{Re}_2\text{I}_8]^{2-}$ with monodentate phosphines in benzene appeared to be similar to those of $[\text{Re}_2\text{Cl}_8]^{2-}$ giving the same kinetic products for the respective ligands. For PMe_3 we have isolated the edge-sharing bioctahedral dirhenium(III) complex, 1,3,5,7- $\text{Re}_2(\mu\text{-I})_2\text{I}_4(\text{PMe}_3)_4$ (**1b**), with a long Re...Re separation of 4.274(1) Å and a *cis*, *cis* disposition of phosphine ligands. In the case of PEt_3 we have found a kinetic product with $\text{Re}_2\text{I}_6\text{P}_2$ stoichiometry and a Re_2^{5+} core, namely $[\text{Bu}_4\text{N}][\text{Re}_2\text{I}_6(\text{PEt}_3)_2]$ (**3c**). No intermediates have been detected for the PMe_2Ph and PEt_2Ph ligands. However, it is clear that those kinetic products are significantly less stable for iodides than for chlorides and their disproportionation products appear to be different. Thus, for PMe_3 and PMe_2Ph those are 1,3,6,8- $\text{Re}_2\text{I}_4(\text{PR}_3)_4$ versus 1,2,7- $\text{Re}_2\text{Cl}_5(\text{PR}_3)_3$. The reactivity of these intermediates is also different: the reduction of $\text{Re}_2\text{X}_6(\text{PMe}_3)_4$ gives *trans* products of the Re_2^{5+} and Re_2^{4+} for $\text{X} = \text{I}$ (**1d**, **1a**) versus the corresponding *cis* complexes for $\text{X} = \text{Cl}$ [5g].

We believe that the different results of substitutions on the $[\text{Re}_2\text{I}_8]^{2-}$ ion and the $[\text{Re}_2\text{Cl}_8]^{2-}$ ion can be well accounted for by recognizing that Cl^- has a higher *trans* effect than I^- . Thus, the order of *trans* effects is



Scheme 2.

$\text{Cl}^- > \text{PR}_3 > \text{I}^-$. The consequences of this are shown in Scheme 2. Both $[\text{Re}_2\text{X}_8]^{2-}$ ions first react in the same way with two molecules of PR_3 to give 1,7- $\text{Re}_2\text{X}_6\text{P}_2$ intermediates, but then there is a difference depending on whether $\text{X}^- = \text{Cl}^-$ or I^- . The higher *trans* effect of Cl^- leads to the successive formation of 1,2,7 and 1,2,7,8 products, while the lower *trans* effect of I^- leads to the formation of 1,3,6 followed by 1,3,6,8 products. There are, of course, further complications, but this much at least seems to make sense.

4. Supplementary material

Crystallographic data (excluding structure factors) for the structures reported in this paper have been deposited with the Cambridge Crystallographic Data Center, CCDC Nos. 141439–141445 for **1a**· CH_2Cl_2 , **1b**· $2\text{C}_6\text{H}_6$, **1d**, **2a**, **3c**· $(1/3)\text{C}_6\text{H}_6$, **4a**, and $[\text{Re}_2\text{Cl}_4(\text{PMe}_3)_4]\text{I}\cdot\text{CH}_2\text{Cl}_2$, respectively. Copies of the data can be obtained free of charge from The Director, CCDC, 12 Union Road, Cambridge CB2 1EZ, UK (fax: +44-1223-336033; e-mail: deposit@ccdc.cam.ac.uk or www: <http://www.ccdc.cam.ac.uk>).

Acknowledgements

We acknowledge support by the National Science Foundation.

References

- [1] F.A. Cotton, R.A. Walton, Multiple Bonds between Metal Atoms, 2nd edn, Oxford University Press, Oxford, 1993.
- [2] H.D. Glicksman, R.A. Walton, Inorg. Chem. 17 (1978) 3197.
- [3] P. Brant, D.J. Salmon, R.A. Walton, J. Am. Chem. Soc. 100 (1978) 4424.
- [4] (a) J.R. Ebner, R.A. Walton, Inorg. Chem. 14 (1975) 1987. (b) K.R. Dunbar, R.A. Walton, Inorg. Chem. 24 (1985) 5. (c) F.A. Cotton, Inorg. Chem. 37 (1998) 5710.
- [5] (a) F.A. Cotton, E.V. Dikarev, M.A. Petrukhina, J. Am. Chem. Soc. 119 (1997) 12 541. (b) F.A. Cotton, E.V. Dikarev, M.A. Petrukhina, Inorg. Chem. 37 (1998) 1949. (c) F.A. Cotton, E.V. Dikarev, M.A. Petrukhina, Inorg. Chem. 37 (1998) 6035. (d) F.A. Cotton, E.V. Dikarev, M.A. Petrukhina, Inorg. Chem. Commun. 2 (1999) 28. (e) F.A. Cotton, E.V. Dikarev, M.A. Petrukhina, Inorg. Chem. 38 (1999) 3384. (f) F.A. Cotton, E.V. Dikarev, M.A. Petrukhina, Inorg. Chem. 38 (1999) 3899. (g) F.A. Cotton, E.V. Dikarev, M.A. Petrukhina, in preparation.
- [6] (a) W. Preetz, L. Rudzik, Angew. Chem., Int. Ed. Engl. 18 (1979) 150. (b) F.A. Cotton, L.M. Daniels, K. Vidyasagar, Polyhedron 7 (1988) 1667.
- [7] (a) A. Fürstner, Angew. Chem., Int. Ed. Engl. 32 (1993) 164. (b) M.A. Schwindt, T. Lejon, L.S. Hegedus, Organometallics 9 (1990) 2814.
- [8] F.A. Cotton, E.V. Dikarev, X. Feng, Inorg. Chim. Acta 237 (1995) 19.
- [9] J. Pflugrath, A. Messerschmitt, MADNES, Munich Area Detector (New EEC) System, version EEC 11/9/89, with enhancements by Enraf-Nonius Corp., Delft, The Netherlands. A description of MADNES appears in: A. Messerschmitt, J. Pflugrath, J. Appl. Crystallogr. 20 (1987) 306.
- [10] (a) W. Kabsch, J. Appl. Crystallogr. 21 (1988) 67. (b) W. Kabsch, 21 (1988) 916.
- [11] SHELXTL V.5; Siemens Industrial Automation Inc., Madison, WI, 1994.
- [12] G.M. Sheldrick, in: H.D. Flack, L. Parkanyi, K. Simon (Eds.), Crystallographic Computing 6, Oxford University Press, Oxford, 1996, p. 111.
- [13] (a) F.A. Cotton, A.C. Price, K. Vidyasagar, Inorg. Chem. 29 (1990) 5143. (b) F.A. Cotton, E.V. Dikarev, Inorg. Chem. 35 (1996) 4738.
- [14] D.R. Root, C.H. Blevins, D.L. Lichtenberger, A.P. Sattelberger, R.A. Walton, J. Am. Chem. Soc. 108 (1986) 953.
- [15] F.A. Cotton, J.G. Jennings, A.C. Price, K. Vidyasagar, Inorg. Chem. 29 (1990) 4138.
- [16] F.A. Cotton, K.R. Dunbar, L.R. Falvello, M. Tomas, R.A. Walton, J. Am. Chem. Soc. 105 (1983) 4950.

- [17] (a) F.A. Cotton, W.A. Wojtczak, *Gazz. Chim. Ital.* 123 (1993) 499. (b) F.A. Cotton, M.P. Diebold, P.A. Kibala, *Inorg. Chem.* 27(1988) 799. (c) J.H. Wengrovius, R.R. Schrock, C.S. Day, *Inorg. Chem.* 20 (1981) 1844. (d) M.E. Riehl, S.R. Wilson, G.S. Girolami, *Inorg. Chem.* 32 (1993) 218.
- [18] F.A. Cotton, M. Shang, W.A. Wojtczak, *Inorg. Chem.* 30 (1991) 3670.
- [19] S.I. Troyanov, A. Meetsma, J.H. Teuben, *Inorg. Chim. Acta* 271 (1998) 180.
- [20] R.A. Walton, *Prog. Inorg. Chem.* 16 (1972) 1.